

1 **Leaf-GP: An Open and Automated Software Application for Measuring Growth Phenotypes for**
2 **Arabidopsis and Wheat**

3

4 Ji Zhou^{1,2,3,*}, Christopher Applegate¹, Albor Dobon Alonso², Daniel Reynolds¹, Simon Orford², Michal
5 Mackiewicz³, Simon Griffiths², Steven Penfield², and Nick Pullen²

6

7 ¹Earlham Institute, Norwich Research Park, Norwich UK

8 ²John Innes Centre, Norwich Research Park, Norwich UK

9 ³University of East Anglia, Norwich Research Park, Norwich UK

10 *Correspondence: ji.zhou@earlham.ac.uk

11

12 Authors email addresses:

- 13 • Ji Zhou, Ji.Zhou@earlham.ac.uk or ji.zhou@jic.ac.uk
- 14 • Christopher Applegate, Christopher.Applegate@earlham.ac.uk
- 15 • Albor Dobon, Albor.Dobon@jic.ac.uk
- 16 • Daniel Reynolds, Daniel.Reynolds@earlham.ac.uk
- 17 • Simon Orford, simon.orford@jic.ac.uk
- 18 • Michal Mackiewicz, M.Mackiewicz@uea.ac.uk
- 19 • Simon Griffiths, simon.griffiths@jic.ac.uk
- 20 • Steven Penfield, steven.penfield@jic.ac.uk
- 21 • Nick Pullen, Nick.Pullen@jic.ac.uk

22

23

24 **Abstract**

25 **Background:** Plants demonstrate dynamic growth phenotypes that are determined by genetic and
26 environmental factors. Phenotypic analysis of growth features over time is a key approach to understand
27 how plants interact with environmental change as well as respond to different treatments. Although the
28 importance of measuring dynamic growth traits is widely recognised, available open software tools are
29 limited in terms of batch processing of image datasets, multiple trait analysis, software usability and
30 cross-referencing results between experiments, making automated phenotypic analysis problematic.

31
32 **Results:** Here, we present Leaf-GP (Growth Phenotypes), an easy-to-use and open software application
33 that can be executed on different platforms. To facilitate diverse scientific user communities, we provide
34 three versions of the software, including a graphic user interface (GUI) for personal computer (PC)
35 users, a command-line interface for high-performance computer (HPC) users, and an interactive *Jupyter*
36 *Notebook* (also known as the iPython Notebook) for computational biologists and computer scientists.
37 The software is capable of extracting multiple growth traits automatically from large image datasets.
38 We have utilised it in *Arabidopsis thaliana* and wheat (*Triticum aestivum*) growth studies at the
39 Norwich Research Park (NRP, UK). By quantifying growth phenotypes over time, we are able to
40 identify diverse plant growth patterns based on a variety of key growth-related phenotypes under varied
41 experimental conditions.

42
43 As Leaf-GP has been evaluated with noisy image series acquired by different imaging devices and still
44 produced reliable biologically relevant outputs, we believe that our automated analysis workflow and
45 customised computer vision based feature extraction algorithms can facilitate a broader plant research
46 community for their growth and development studies. Furthermore, because we implemented Leaf-GP
47 based on open Python-based computer vision, image analysis and machine learning libraries, our
48 software can not only contribute to biological research, but also exhibit how to utilise existing open
49 numeric and scientific libraries (including Scikit-image, OpenCV, SciPy and Scikit-learn) to build
50 sound plant phenomics analytic solutions, efficiently and effectively.

51
52 **Conclusions:** Leaf-GP is a comprehensive software application that provides three approaches to
53 quantify multiple growth phenotypes from large image series. We demonstrate its usefulness and high
54 accuracy based on two biological applications: (1) the quantification of growth traits for *Arabidopsis*
55 genotypes under two temperature conditions; and (2) measuring wheat growth in the glasshouse over
56 time. The software is easy-to-use and cross-platform, which can be executed on Mac OS, Windows and
57 high-performance computing clusters (HPC), with open Python-based scientific libraries preinstalled.
58 We share our modulated source code and executables (.exe for Windows; .app for Mac) together with
59 this paper to serve the plant research community. The software, source code and experimental results
60 are freely available at <https://github.com/Crop-Phenomics-Group/Leaf-GP/releases>.

61
62 **Keywords:** Growth phenotypes, automated trait analysis, feature extraction, computer vision, software
63 engineering, *Arabidopsis*, wheat
64

65 Background

66 Plants demonstrate dynamic growth phenotypes that are determined by genetic and environmental
67 factors [1–3]. Phenotypic features such as relative growth rates (RGR), vegetative greenness and other
68 morphological characters are popularly utilised by researchers in order to quantify how plants interact
69 with environmental changes (i.e. GxE) [4–6]. In particular, to assess the growth and development in
70 response to various experimental treatments, growth phenotypes (e.g. leaf area, canopy size and leaf
71 numbers) are considered as key measurements [7–12], indicating the importance of dynamically scoring
72 differences of growth related traits between experiments. To accomplish the above tasks, high quality
73 image-based growth data need to be collected from many biological replicates over time [13,14], which
74 is then followed by manual, semi-automated, or automated trait analysis [15,16]. However, the current
75 bottleneck lies in how to extract meaningful results from our increasing phenotypic data, effectively
76 and efficiently [14,17].
77

78 To facilitate the quantification of dynamic growth traits, a range of imaging hardware and software
79 have been developed. We summarise some representative tools as follows:
80

- 81 • LeafAnalyser [18] uses image-processing techniques to measure leaf shape variation as well as
82 record the position of each leaf automatically.
- 83 • GROWSCREEN [12] quantifies dynamic seedling growth under altered light conditions.
- 84 • GROWSCREEN FLUORO [19] measures leaf growth and chlorophyll fluorescence to detect
85 stress tolerance.
- 86 • LemnaGrid [20] integrates image analysis and rosette area modelling to assess genotype effects
87 for *Arabidopsis*.
- 88 • Leaf Image Analysis Interface (LIMANI) [21] segments and computes venation patterns of
89 *Arabidopsis* leaves.
- 90 • Rosette Tracker [22] provides an open Java-based image analysis solution to evaluate plant-
91 shoot phenotypes to facilitate the understanding of *Arabidopsis* genotype effects.
- 92 • PhenoPhyte [23] semi-automates the quantification of various 2D leaf traits through a web-
93 based software application.
- 94 • OSCILLATOR [24] analyses rhythmic leaf growth movement using infrared photography
95 combined with wavelet transformation in mature plants.
- 96 • HPGA (a high-throughput phenotyping platform for plant growth modelling and functional
97 analysis) [5], which produces plant area estimation and growth modelling and analysis to high-
98 throughput plant growth analysis.
- 99 • LeafJ [25] provides an ImageJ plugin to semi-automate leaf shape measurement.
- 100 • Integrated Analysis Platform (IAP) [16] is an open framework that performs high-throughput
101 plant phenotyping based on the LemnaTec system.
- 102 • Easy Leaf Area [26] uses colour-based feature to differentiate and measure leaves from their
103 background using a red calibration area to replace scale measurement.
- 104 • Phytotyping^{4D} [27] employs a light-field camera to simultaneously provide a focus and a depth
105 image so that distance information from leaf surface can be quantified.
- 106 • Leaf Angle Distribution Toolbox [28] is a Matlab-based software package for quantifying leaf
107 surface properties via 3D reconstruction from stereo images.
- 108 • MorphoLeaf [29] is a plug-in for the Free-D software to perform analysis of morphological
109 features of leaves with different architectures.
- 110 • rosettR [30] is a high-throughput phenotyping protocol for measuring total rosette area of
111 seedlings grown in plates.
- 112 • A real-time machine learning based classification phenotyping framework [31] can extract leaf
113 canopy to rate soybean stress severity.

114
115 While many hardware and software solutions have been created, the threshold for employing the
116 existing tools for measuring growth phenotypes is still relatively high. This is due to many analytic
117 software solutions that are either customised for specific hardware platforms (e.g. LemnaTec), or relied

118 on proprietary or specialised software platforms (e.g. Matlab), restricting the accessibility for smaller
119 or not well-funded laboratories to utilise the existing solutions [22]. Hence, data annotation, phenotypic
120 analysis, and results cross-referencing are still frequently done manually in many laboratories, which is
121 time consuming and prone to errors [21].

122

123 Available open software tools are also limited in terms of batch processing, multiple trait analysis,
124 and software usability, making automatic phenotypic analysis problematic [30]. In order to provide an
125 open analytics software solution to serve a broader plant research community, we developed Leaf-GP
126 (Growth Phenotypes), an open-source and easy-to-use software solution that can be easily setup for
127 automated analysis using the community driven Python-based scientific and numeric libraries. After
128 continuous development and testing, Leaf-GP can now extract and compare key growth phenotypes
129 reliably from large image series. Some of the growth-related traits are projected leaf area (mm^2), leaf
130 perimeter (mm), canopy length and width (mm), leaf canopy area (mm^2), stockiness (%), compactness
131 (%), leaf numbers and greenness (0-255). We demonstrate its high accuracy and usefulness through
132 experiments using *Arabidopsis thaliana* and *Paragon* wheat (a UK spring wheat variety). The software
133 can be executed on most of the mainstream operating systems with Python and Anaconda distribution
134 preinstalled. More importantly, we followed the open software design strategy, which means our work
135 is expandable and new functions or procedures for other plant species can be easily added.

136

137 **Methods**

138 **Applying Leaf-GP to plant growth studies**

139 Figure 1 illustrates how Leaf-GP was applied to quantify growth phenotypes for *Arabidopsis* rosettes
140 and *Paragon* wheat over time. To improve the software flexibility, Leaf-GP was designed to accept
141 both RGB (a red, green and blue colour model) and infrared (sensitive to short-wavelength infrared
142 radiation at around 880nm) images acquired by a range of devices, including a fixed imaging platform
143 using a Nikon D90 digital camera (Fig. 1a), smartphones (e.g. an iPhone, Fig. 1b), or a mobile version
144 CropQuant [32] equipped with either a *Pi* NoIR (no infrared filter) sensor or an RGB sensor (Fig. 1c).
145 When taking pictures, users need to ensure that the camera covers the regions of interest (ROI), i.e. a
146 whole tray (Fig. 1d) or a pot region (Fig. 1e). Red circular stickers (4mm in radius in our case) shall be
147 applied to the four corners of a tray or a pot (Fig. 1b). In doing so, Leaf-GP can extract ROI from a
148 given raw image and then convert measurements from pixels to metric units (i.e. millimetre, mm). Both
149 raw and processed image data can be loaded and saved by Leaf-GP on personal computers (PCs), HPC,
150 or cloud-based computing storage (Figs. 1f&g).

151

152 As different research groups may have access to dissimilar computing infrastructures, we developed
153 three versions of Leaf-GP to enhance the accessibility of the software: (1) for users utilising HPC
154 clusters, a Python-based script was developed to perform high-throughput trait analysis through a
155 command-line interface (Fig. 1h), which requires relevant scientific and numeric libraries such as SciPy
156 [33], computer vision (i.e. the Scikit-image library [34] and the OpenCV library [35]), and machine
157 learning libraries (i.e. the Scikit-learn library [36]) pre-installed on the clusters; (2) for users working
158 on desktop PCs, a GUI-based (graphic user interface) software application was developed to incorporate
159 batch image processing, multiple trait analysis, and results visualisation in a user-friendly window (Fig.
160 1i); and, (3) for computational biologists and computer scientists who are willing to exploit our source
161 code, we created an interactive *Jupyter Notebook* (Fig. 1j, also known as the iPython Notebook, see
162 Additional File 1) to explain our multilevel trait analysis workflow and how to modulate code to
163 improve algorithm readability. In particular, we have enable the *Notebook* version to process large
164 image series via a *Jupyter* server, which means users can carry out batch image processing directly
165 using the Notebook version. Due to software distribution licensing issues, we recommend users to
166 install the Anaconda Python distribution (Python 2.7 version) and OpenCV (v2.4.11) libraries before
167 using Leaf-GP. Application File 2 explains the step-by-step procedure of how to install Python and
168 necessary libraries for our software.

169

170 After trait analysis, two types of output results are generated. First, *processed images* (Fig. 1k), which
171 includes pre-processing results, calibrated images, colour clustering, and figures exhibiting key growth
172 traits such as leaf outlines, leaf skeletons, detected leaves, and leaf canopy (Additional File 3). Second,
173 *a CSV file* (comma-separated values, Fig. 1l), containing image name, experimental data, pot ID, pixel-
174 to-mm ratio, and biologically relevant outputs including projected leaf area (mm²), leaf perimeter,
175 canopy length and width (in mm), stockiness (%), leaf canopy size (mm²), leaf compactness (%), the
176 number of leaves, and vegetative greenness (Additional File 4).
177

178 **The GUI of Leaf-GP**

179 As plant researchers commonly use PCs for their analyses, we develop the Leaf-GP GUI version based
180 on Python's native GUI package, Tkinter [37]. The version can operate on different platforms (e.g.
181 Windows and Mac OS) and the default resolution of the main window is set to 1024x768 pixels, so that
182 it can be compatible with earlier operating systems (OS) such as Windows 7. Figure 2 illustrates how
183 to utilise the GUI window to process multiple growth image series (five series were imported with four
184 processed). A high-level analysis workflow of Leaf-GP is presented in Figure 2a, containing five steps:
185 (1) data selection, (2) image pre-processing, (3) global ROI segmentation (i.e. at image level), (4) local
186 trait analysis (i.e. at the pot level), and (5) results output. To explain functions and procedures developed
187 for the workflow, we also prepared a detailed UML (unified modelling language) activity diagram [38]
188 that elucidates stepwise actions, which includes software engineering activities such as choice, iteration,
189 and concurrency to enable the batch processing of large image datasets (Additional File 5).
190

191 Figure 2b shows five self-explanatory sections designed to integrate the above analysis steps into the
192 GUI version of the software, including: Data Input, Colour Clustering Setting, Series Processing,
193 Processing Log (a hidden section), and Results Section. To analyse one or multiple image series, users
194 just need to follow these sections sequentially. Also, a number of information icons (coloured blue)
195 have been included to explain how to enter input parameters. Figure 2b demonstrates a screenshot of
196 Leaf-GP after it has finished processing four image series.
197

198 *Section 1 – Data Input*

199 To simplify the data input phase, we only require users to enter essential information regarding their
200 images and associated experiments. To complete the section (Fig. 2c), the user first needs to choose a
201 directory ("Image Dir.") which contains captured image series. Then, the user shall enter parameters in
202 the "Row No." and "Column No." input boxes to define the layout of the tray used in the experiment
203 as well as "Ref. Radius (mm)" to specify the radius of the red stickers. Finally, the user needs to select
204 from "Plant Species" and "Read Exp. Data" dropdowns. All inputs will be verified upon entry to ensure
205 only valid parameters can be submitted to the core algorithm.
206

207 In particular, the "Read Exp. Data" dropdown determines how Leaf-GP reads experiment metadata
208 such as imaging date, treatments and genotypes. For example, choosing the "From Image Name" option
209 allows the software to read information from the filename, selecting the "From Folder Name" option
210 will extract metadata from the directory name, whereas the "No Metadata Available" selection will
211 group all images as an arbitrary series for trait analysis. This option allows users to analyse images that
212 are *not* following any data annotation protocols. Although not compulsory, we developed a simple
213 naming convention protocol (Additional File 6) to assist users to annotate image names or folder names
214 tailored for Leaf-GP.
215

216 *Section 2 – Colour Clustering Setting*

217 Once the data input phase is completed, the user can click the 'Load' button to initiate series sorting,
218 which will populate the *Colour Clustering Setting* section automatically (Fig. 2d). A sample image from
219 the midpoint of a given series will be chosen by the software, i.e. the image represents the colour groups
220 in the middle of the plant growth. The image is then downsized and processed by a simple k-means
221 method [36], producing a clustering plot and a *k* value that populates in the "Pixel Groups" input box.
222 The user can override the *k* value in the "Pixel Groups" input box; however, to reduce the computational
223 complexity, Leaf-GP only accepts a maximum value of 10 (i.e. 10 representative colour groups) and a

224 minimum value of 3 (i.e. three colour groups) when conducting trait analysis. The generated k value
225 (between 3 and 10) will be passed to the core analysis algorithm when the batch processing starts.
226

227 *Sections 3&4 – Series Processing*

228 In the *Series Processing* section (Fig. 2e), the software fills the processing table with information that
229 can help users identify different experiments, including experiment reference (“Exp. Ref.”), the tray
230 number (“Tray No.”), and the number of images in a series (“No. Images”). To improve the appearance
231 of the table, each column is resizable. Checkboxes are prepended to each recognised series. Users can
232 toggle one or multiple checkboxes to specify how many experiments will be processed. If the ‘No
233 Metadata Available’ option is selected (see the *Data Input* section), information such as “Exp. Ref.”
234 and “Tray No.” will not be populated.
235

236 The initial status of each processing task (“Status”) is *Not Processed*, which will be updated constantly
237 during the image analysis. When more than one experiment is selected, Python’s thread pool executor
238 function will be applied, so that these experiments can be analysed simultaneously in multiple cores in
239 the central processing unit (CPU). We have limited up to *three* analysis threads (see the right of Fig.
240 2e), because many Intel processors comprise *four* physical cores and conducting parallel computing can
241 have a high demand of computing resources (e.g. storage, CPU and memory), particularly during the
242 batch processing when raw image datasets are big.
243

244 Once the processing table is filled, the user can click the ‘Run Analysis’ button to commence the
245 analysis. Figure 2b shows the screenshot when five experiments (i.e. five image series) are recognised
246 and four of them are analysed. Due to the multi-task design of Leaf-GP, we only allowed three series
247 running in parallel. Throughout the analysis, the ‘Status’ column will be continually updated, indicating
248 how many images have been processed. It is important to note that, although Leaf-GP was designed for
249 parallel computing, some functions used in the core algorithm are not thread-safe, indicating they can
250 only be executed by one thread at a time. Because of this limit, we have utilised lock synchronisation
251 mechanisms to protect code blocks (i.e. procedures or functions), so that these thread-unsafe blocks can
252 only be executed by one thread at a time. In addition to the processing status, more analysis information
253 can be viewed by opening the *Processing Log* section (to the right of Fig. 2e), which can be displayed
254 or hidden by clicking the ‘Show/Hide Processing Log’ button on the main window.
255

256 *Section 5 – Results*

257 When all processing tasks are completed, summary information will be appended to the Results section,
258 including processing ID and a link to the result folder which contains the CSV file and all processed
259 images (“Result Dir.”). Depending on which species (i.e. *Arabidopsis* rosette or wheat) is selected, trait
260 plots will be generated to show key growth phenotypes (e.g. the projected leaf area, leaf perimeter, leaf
261 canopy size, leaf compactness, and leaf numbers) by clicking on the associated cell in the Results table
262 (Fig. 2f). The range of phenotype measurements is also listed in the *Results* section. The GUI version
263 also saves processing statistics, for example, how many images have been successfully analysed and
264 how many images have been declined, together with related error or warning messages in a log file for
265 debugging purposes.
266

267 **Core trait analysis algorithms**

268 Multiple trait analysis of *Arabidopsis* rosettes and wheat plants is the core part of Leaf-GP. Not only
269 does it utilise advance computer vision algorithms for automated analysis, it also encapsulates feature
270 extraction and phenotypic analysis methods that are biologically relevant to growth phenotypes. In the
271 following sections, we explain the core analysis algorithm in detail.
272

273 *Step 2 – Pre-processing and calibration*

274 Different imaging devices, camera positions and even lighting conditions can cause quality variance
275 during image acquisition. Hence, it is important to calibrate images before conducting automated trait
276 analysis. We developed a pre-processing and calibration procedure as shown in Figure 3. We first
277 resized each image (Fig. 3a) to a fixed resolution so that the height (i.e. y-axis) of all images in a given

278 series could be fixed. A `rescale` function in Scikit-image was used to dynamically transform the
279 image height to 1024 pixels (Fig. 3b). After that, we created a `RefPoints` function (*Function_2* in
280 Additional File 1) to detect red circular markers attached to the corners of a tray or a pot region. To
281 extract these markers robustly under different illumination conditions, we designed $g(x, y)$, a multi-
282 thresholding function to segment red objects derived from a single-colour extraction approach [39]. The
283 function defines which pixels shall be retained (intensity is set to 1) and which pixels shall be discarded
284 (intensity is set to 0) after the thresholding:
285

$$286 \quad g(x, y) = \begin{cases} 1, & \text{if } f_R(x, y) > 125 \text{ and } f_B(x, y) < 225 \text{ and } (f_R(x, y) - f_G(x, y)) > 50 \\ 0, & \text{otherwise} \end{cases} \quad (1)$$

287 where $f_R(x, y)$ is the red channel of a colour image, $f_B(x, y)$ represents the blue channel and $f_G(x, y)$
288 the green channel. The result of the function is saved in a reference binary mask.
289

290
291 We then used the `regionprops` function in Scikit-image to measure morphological features of the
292 reference-point mask to filter out false positive items. For example, if an object's area, eccentricity or
293 solidity readings do *not* fit into the characteristics of a circle, this object will be discarded. After this
294 step, only genuine circular objects are retained (Fig. 3c) and the average radius (in pixels) of these
295 circular objects is converted to mm units (the radius of the red markers is 4mm). To extract the tray
296 region consistently, we developed a tailored algorithm called `PerspectiveTrans_2D` (*Function_5*
297 in Additional File 1), using `getPerspectiveTransform` and `warpPerspective` functions in
298 OpenCV to retain the region that is enclosed by the red markers (Fig. 3d). Finally, we employed a non-
299 local means denoising function called `fastNlMeansDenoisingColored` in OpenCV to smooth
300 leaf surface for the following global leaf ROI segmentation (Fig. 3e).
301

302 *Step 3 – Global leaf ROI segmentation*
303 Besides imaging related issues, changeable experimental settings could also cause issues for automated
304 trait analysis. Figures 4a-d illustrate a number of problems we have encountered whilst developing
305 Leaf-GP. For example, the colour and texture of the soil surface can change considerably between
306 different experiments, especially when gritty compost and other soil types are used (Figs. 4a&b);
307 sometimes plants are *not* positioned in the centre of a pot (Fig. 4b), indicating leaves that cross over to
308 adjacent pots should be segmented; algae growing on the soil has caused false detection due to their
309 bright green colour (Figs. 4c&d); finally, destructive harvest for weighing biomass could occur from
310 time to time throughout an experiment, indicating the core analysis algorithm needs to handle random
311 pot disruption robustly (Fig. 4d). To address the above technical challenges, we developed a number of
312 computer vision and simple machine-learning algorithms based on open scientific libraries. Results of
313 our software solutions integrated in Leaf-GP can be seen to the right of Figures 4a-d.
314

315 The first approach we developed is to establish a consistent approach to extract pixels containing high
316 values of greenness (i.e. leaf regions) from an RGB image robustly. Using a calibrated image, we
317 computed vegetative greenness $G_V(x, y)$ [13] based on excessive greenness $Ex_G(x, y)$ and excessive
318 red $Ex_R(x, y)$ indices. The pseudo vegetative greenness image (G_V , Figure 4e) is produced by equation
319 2, based on which we implemented a `compute_greenness_img` function (*Function_8* in
320 Additional File 1) to transfer an RGB image into a G_V picture. Excessive greenness is defined by
321 equation 3 and excessive red is defined by equation 4:
322

$$323 \quad G_V(x, y) = Ex_G(x, y) - Ex_R(x, y) \quad (2)$$

$$324 \quad Ex_G(x, y) = 2 * f_G(x, y) - f_R(x, y) - f_B(x, y) \quad (3)$$

$$325 \quad Ex_R(x, y) = 1.4 * f_R(x, y) - f_B(x, y) \quad (4)$$

326
327 where $f_R(x, y)$ is the red channel of a colour image, $f_B(x, y)$ represents the blue channel, and $f_G(x, y)$
328 the green channel.
329

330 After that, we applied a simple unsupervised machine learning algorithm called **KMeans** (default $k =$
331 8 was used, assuming 8 representative colour groups in a given image) and **KMeans.fit** in Scikit-
332 learn to estimate how many colour groups can be classified (Fig. 4f, *Function_8.1* in Additional File 1).
333 We chose a median threshold (red dotted line) to segment the colour clustering result and obtained the
334 k value to represent the number of colour groups (Fig. 4g). Also, this process has been integrated into
335 the GUI version (i.e. the *Colour Clustering Setting* section). Utilising the k value (e.g. $k = 4$, Fig. 4g),
336 we designed a **kmeans_cluster** function (*Function_9* in Additional File 1) to classify the pseudo
337 vegetative greenness picture, highlighting greenness values in red pixels (Fig. 4h). A global adaptive
338 Otsu thresholding [40] was used to generate an image level leaf ROI binary mask (Fig. 4i). However,
339 the simple machine learning approach could produce miss-detected objects due to complicated colour
340 presentations during the plant growth period (e.g. Figs. 4a-d). For example, the k-means approach
341 performed well when the size of the plants is between 25-75% of the size of a pot, but created many
342 false detections when leaves are tiny or the background is complicated. Hence, we designed another
343 approach to improve the detection based on the k-means approach.
344

345 We employed Lab colour space [41], which incorporates lightness and green-red colour opponents to
346 refine the detection. We created an internal procedure called **LAB_Img_Segmentation** (*Function_7*
347 in Additional File 1) to transfer RGB images into Lab images using the **color.rgb2lab** function in
348 Scikit-image, based on which green pixels were featured in a non-linear fashion (Fig. 4j). Again, a
349 global adaptive Otsu thresholding was applied to extract leaf objects and then a Lab-based leaf region
350 mask (Fig. 4k). Finally, we combined the Lab-based mask with the k-means mask as the output of the
351 phase of global leaf ROI segmentation.
352

353 *Step 4.1 – Pot level segmentation*

354 To measure growth phenotypes in a given pot over time, plants within each pot need to be monitored
355 over time. Using the calibrated images, we have defined the tray region, based on which we constructed
356 the pot framework in the tray. To accomplish this task, we designed an iterative layout drawing method
357 called **PotSegmentation** (*Function_5* in Additional File 1) to generate anti-aliased lines using the
358 **line_aa** function in Scikit-image to define the pot layout (Fig. 5a).
359

360 After constructing the framework, we segmented the leaf growth image into a number of sub-images
361 (Fig. 5b), so that plant can be analysed locally, at the pot level. We developed an iterative analysis
362 approach to go through each pot with the sequence presented in Figure 5c. Within each pot, we
363 conducted a local leaf detection method. For example, although combining leaf masks produced by the
364 machine learning (Fig. 4i) and the Lab colour space (Fig. 4k) approaches, some false positive objects
365 may still remain (Fig. 5d). The local leaf detection can enable us to employ pot-level contrast and
366 intensity distribution [42], weighted image moments [43], texture descriptor [44], and leaf positional
367 information to examine each sub-image to refine the leaf detection (Fig. 5e). This local feature selection
368 method (detailed in the following sections) can also help us decrease the computational complexity (i.e.
369 memory and computing time), as analysis is carried out within smaller sub-images.
370

371 *Step 4.2 – Local multiple trait measurements*

372 Utilising the refined local leaf masks at the pot level (Fig. 6a), a number of growth phenotypes could
373 be quantified reliably. Some of them are enumerated briefly as follows:
374

- 375 1) “Projected Leaf Area (mm^2)” measures the area of an overhead projection of the plant in a pot.
376 While implementing the function, the **find_contours** function in Scikit-image is used to outline
377 the leaf region (coloured yellow in Fig. 6b). Green pixels enclosed by the yellow contours are
378 totalled to compute the size of the projected leaf area (Fig. 6c). Pixel-based quantification is then
379 converted to mm units based on the pixel-to-mm exchange rate. This trait is a very reliable
380 approximation of the three-dimensional (3D) leaf area and has been used in many growth studies
381 [20,22,45].
382

383 2) “Leaf Perimeter (mm)” is calculated based on the length of the yellow contour line that encloses
 384 the detected leaf region. Again, pixel-based measurements are converted to mm units, which are
 385 then used to compute the size change of a plant over time.

386

387 3) “Daily Relative Growth Rate (%)” (Daily RGR) quantifies the speed of plant growth. Derived from
 388 the RGR trait described previously [19,46], the Daily RGR here is defined by equation 5:

389

$$390 \quad \frac{1}{(t_2-t_1)} * (\ln(Area_{2_i}) - \ln(Area_{1_i})/\ln(Area_{1_i}) \quad (5)$$

391

392 where \ln is natural logarithm, $Area_{1_i}$ is the projected leaf area in pot i in the previous image,
 393 $Area_{2_i}$ is the leaf area in pot i in the current image, and $(t_2 - t_1)$ is the duration (in days) between
 394 the two consecutive images.

395

396 4) “Leaf Canopy (mm²)” expresses the plant canopy region that is enclosed by a 2D convex hull in a
 397 pot [19,20,22]. The convex hull was generated using the `convex_hull_image` function in
 398 Scikit-image, enveloping all pixels that belong to the plant with a convex polygon [47]. Figure 6d
 399 presents all convex hulls created in a given tray. As described previously [19], this trait can be used
 400 to define the coverage of the leaf canopy region as well as how the petiole length changes during
 401 the growth period.

402

403 5) “Stockiness (%)” is calculated based on the ratio between the plant projected area and the leaf
 404 perimeter (Fig. 6e). It is defined as $(4\pi * Area_i)/(2\pi * R_i)^2$, where $Area_i$ is the projected leaf
 405 area detected in pot i and R_i is the longest radius (i.e. major axis divided by 2) of the convex hull
 406 polygon in pot i . This trait (0-100%) has been used to measure how serrated a plant is, which can
 407 also indicate the circularity of the leaf region (e.g. a perfect circle will score 100%).

408

409 6) “Leaf Compactness (%)” is computed based on the ratio between the projected leaf area and the
 410 area of the convex hull enclosing the plant [20,22]. Figure 6f shows how green leaves are enclosed
 411 by yellow convex hull outlines that calculates the leaf compactness trait.

412

413 7) “Greenness” monitors the normalised greenness value (0-255) of the leaf canopy, i.e. the convex
 414 hull region. A rescaled Lab image is used to provide the greenness reading, so that we could
 415 minimise the background noise caused by algae and soil types. Greenness can be used to study plant
 416 growth stages such as vegetation and flowering.

417

418 *Step 4.3 – Leaf number detection*

419 As the number of rosette leaves is popularly used to determine key growth stages for *Arabidopsis* [15],
 420 we therefore designed a leaf structure detection algorithm to provide a consistent reading of traits such
 421 as the number of detected leaves and the number of detected long or large leaves over time. This
 422 algorithm comprises of a 2D topological skeletonisation algorithm (*Function_10* in Additional File 1)
 423 and a leaf outline sweeping method (*Function_11* in Additional File 1).

424

425 Figure 7a demonstrates the result of the skeletonisation approach, which utilises the `skeletonize`
 426 function in Scikit-image to extract 2D skeletons from the leaf masks in each pot. The skeletons can be
 427 used to quantify the structural characteristics of a plant, including the number of leaf tips and branching
 428 points of a plant. For example, we implemented a `find_end_points` function to detect each leaf
 429 tip (i.e. end point) in a plant skeleton using the `binary_hit_or_miss` function in the SciPy library
 430 to match the four possible 2D matrix representations:

431

$$432 \quad \begin{matrix} 0 & 0 & 0 \\ 0 & 1 & 0 \end{matrix} \text{ or } \begin{matrix} 0 & 1 & 0 \\ 0 & 0 & 0 \end{matrix} \text{ or } \begin{matrix} 0 & 0 \\ 0 & 1 \end{matrix} \text{ or } \begin{matrix} 0 & 0 \\ 1 & 0 \end{matrix} \quad (6)$$

433

434 The **find_end_points** function outputs 2D coordinates of end points that correlates with leaf tips
435 (Fig. 7b). Furthermore, the function can be employed for novel trait measurements, for instance, large
436 or long rosette leaves can be identified if they are over 50% or 70% of the final size (Fig. 7c and
437 *Step_4.4.2.7* in Additional File 1). To accomplish this, we evaluated the leaf skeleton as a weighted
438 graph and then treated: (1) the skeleton centroid and end points as *vertices* (i.e. *nodes*), (2) lines between
439 the centre point and end points as *edges*, and (3) the leaf area and the length between vertices as *weights*
440 assigned to each *edge*. Depending on the experiment, if the *weights* are greater than a predefined
441 threshold (i.e. over 15mm in length and 100mm² in leaf size in our case), the associated leaf will be
442 recognised as a long or large leaf.

443
444 As the skeletonisation approach could miss some small leaves if they are close to the plant centroid
445 or partially overlapping with other leaves, we implemented a **leaf_outline_sweeping** procedure
446 to establish another approach to detect the total leaf number based on the distance between the plant
447 centroid and any detected leaf tips. This procedure is based on a published leaf tip identification
448 algorithm [5]. We improved upon the algorithm through utilising the leaf boundary mask (i.e. contour)
449 to reduce the computational complexity. For a given plant, the algorithm generates a distance series that
450 represents the squared Euclidean distances from the plant centroid to its contour, at angles between 0
451 and 359 degrees with a 1-degree interval (for presentation purposes, we only used 15 degree intervals
452 in Fig. 7d). To reduce noise, the algorithm smooths the distance series using a Gaussian kernel (Fig.
453 7e). A peak detection algorithm called **PeakDetect** [48] is integrated in our core analysis algorithm
454 to detect peaks on the distance series (*Step_4.4.2.8* in Additional File 1). The procedure implemented
455 here supports our assumption that the number of peaks can be used to largely represent the number of
456 leaf tips (Figs. 8f&g). When quantifying the total number of leaves, results from both skeleton and
457 outline sweeping approaches are combined to produce a viable measurement.
458

459 Results

460 Leaf-GP can facilitate plant growth studies through automating trait analysis and cross-referencing
461 results between experiments. Instead of merely utilising machine learning algorithms to build neural
462 network architecture for pixel clustering or trait estimates [49], we chose an approach that combines
463 simple unsupervised machine learning and advance computer vision algorithms to establish an efficient
464 analysis workflow. This approach has enabled us to select morphological features that are biologically
465 relevant for conducting meaningful ROI segmentation at both image and pot levels. Here, we exhibit
466 three use cases where Leaf-GP were employed to study key growth phenotypes for *Arabidopsis* rosettes
467 and *Paragon* wheat.
468

469 Use case 1 – Tracking three genotypes in a single tray

470 We applied Leaf-GP to measure growth phenotypes in a tray containing three genotypes *Ler* (wildtype),
471 *spt-2*, and *gai-t6 rga-t2 rgl1-1 rgl2-1 (della4)* at 17°C. Each pot in the tray was monitored and cross-
472 referenced during the experiment. The projected leaf area trait in 24 pots was quantified by Leaf-GP
473 (Fig. 8a) and rosette leaves were measured from stage 1.02 (2 rosette leaves, around 5mm²) to stage 5
474 or 6 (flower production, over 2400mm²), a duration of 29 days after the first image was captured.
475

476 After dividing the quantification into three genotype groups, we used the projected leaf area readings
477 (Fig. 8b) to verify the previously manually observed growth differences between *Ler*, *spt-2*, and *della4*
478 [2,3]. Furthermore, the differences in phenotypic analyses such as leaf perimeter, compactness, leaf
479 number, and daily RGR of all three genotypes can be statistically differentiated (Figs. 8c–f). Particularly
480 for Daily RGR (Fig. 8f), the three genotypes exhibit a wide variety of growth rates that are known to
481 be determined by genetic factors [50]. Based on image series, Leaf-GP can integrate time and treatments
482 (e.g. temperature signalling or chemicals) with dynamic growth phenotypes for cross referencing. We
483 provided the CSV file for *Use Case 1* in Additional File 4, containing trait measurements for each pot
484 over time. The Python script we used to plot and cross-reference either pot- or genotype-based growth
485 phenotypes is provided in Additional File 7, called Leaf-GP plot generator.
486

487 *Use case 2 – Two genotypes under different temperatures*

488 We also used our software to detect differences in rosette growth between *Ler* (wildtype) and *spt-2*
489 grown at different temperatures, i.e. 12°C and 17°C. Utilising the projected leaf area measurements, we
490 observed that temperatures affect vegetative growth greatly on both lines (Fig. 9a). Similar to previously
491 studied [2,3], lower temperatures can have a greater effect on the growth of *spt-2* than *Ler*. Around
492 seven weeks after sowing, the projected leaf area of *spt-2* was around 50% greater on average (1270mm²)
493 compared to *Ler* (820mm²), when grown at 12°C (Fig. 9c). However, when grown in 17 °C, at 36 days-
494 after-sowing *spt-2* had a similar area at around 1200mm², but *Ler* had an area of 1000mm², a much
495 smaller difference.

496
497 As our software can export multiple growth phenotypes, we therefore investigated both linked and
498 independent effects of temperature on wildtype and *spt-2*. For instance, the larger rosette in *spt-2* causes
499 a similar increase in rosette perimeter, canopy length and width, and canopy size. At similar days after
500 sowing, plants of both genotypes grown at 12°C had more compact rosettes than those growing at 17°C
501 (Fig. 9b), and *spt-2* was less compact than *Ler* in general. The number of leaves produced was greater
502 at the warmer temperature (Fig. 9c). This ability to easily export a number of key growth traits of interest
503 is useful and relevant to broader plant growth research. We provided detailed processing results (csv
504 files) for the *Ler* (12°C and 17°C, Additional File 8) and *spt-2* (12°C and 17°C, Additional File 9)
505 experiments. Results including processed images and CSV files for the two experiments can also be
506 downloaded at <https://github.com/Crop-Phenomics-Group/Leaf-GP/releases>.

507
508 *Use case 3 – Monitoring wheat growth*

509 Another application for which Leaf-GP has been designed is to analyse wheat growth images taken in
510 glasshouses or growth chambers. Similarly, red circular stickers are required to attach to the corners of
511 the pot region so that Leaf-GP can extract ROI and traits can be measured in mm units. Figure 10
512 demonstrates a proof-of-concept study demonstrating how Leaf-GP has been applied to measure
513 projected leaf area and leaf canopy size based on *Paragon* (a UK spring wheat) image series taken over
514 a 70-day period in greenhouse, from sprouting (Fig. 10b), to tillering (Fig. 10c), and then from booting
515 (Fig. 10e) to heading (Fig. 10f). With a simple and cheap imaging setting, Leaf-GP can precisely
516 quantify key growth phenotypes for wheat under different experimental conditions. Please note that the
517 leaf counting function in Leaf-GP cannot be reliably applied to quantify wheat leaves, because the
518 complicated plant architecture of wheat plants.

519

520 **Discussion**

521 Different environmental conditions and genetic mutations can impact a plant's growth and development,
522 making the quantification of growth phenotypes a useful tool to study how plants respond to different
523 biotic and abiotic treatments. Amongst many popularly used growth phenotypes, imaging leaf-related
524 traits is a non-destructive and reproducible approach for plant scientists to record plant growth over
525 time. In comparison with many published image analysis software tools for leaf phenotyping, our
526 software provides a comprehensive solution that is capable of extracting multiple traits automatically
527 from large image datasets; and moreover, it can provide traits analysis that can be used to cross reference
528 different experiments. In order to serve a broader plant research community, we designed three versions
529 of Leaf-GP, including a graphic user interface for PC users, a command-line interface for HPC users,
530 and a *Jupyter Notebook* for computational users. We provide all steps of the algorithm design and
531 software implementation, together with raw and processed datasets we produced for our *Arabidopsis*
532 and *Paragon* wheat studies at NRP.

533

534 When developing the software, we particularly considered how to enable different sizes of plant
535 research laboratories to utilise our work for screening large populations of *Arabidopsis* and wheat in
536 response to varied treatments through accessible and low-cost imaging devices. Hence, we paid much
537 attention to software usability (e.g. simple command-line interface or GUI), capability (automatic
538 multiple trait analysis running on different platforms), expandability (open software architecture, new
539 Python-based functions and procedures can be easily added to the software, see the **PeakDetect**

540 procedure in Additional File 1), and biological relevance (i.e. the feature extraction approach and
541 processing results are biological relevant). We trust our software is suitable for studying the growth
542 performance of a large number of plant genotypes and treatments with very limited imaging hardware
543 and software resource requirements.

544
545 The software has been used to evaluate noisy images caused by algae and different soil surfaces such
546 as gritty compost, dry and wet soil types. Still, it can automatically and reliably execute the analysis
547 tasks without users' intervention. To verify Leaf-GP's trait measurements, we have scored manually
548 the key growth phenotypes on the same pots and obtained a correlation coefficient of 0.958. As the
549 software is implemented based on open image analysis, computer vision and machine learning libraries,
550 Leaf-GP can be easily adopted or redeveloped for other experiments. To support computational users
551 to comprehend and share our work, we have provided very detailed comments in our source code.

552
553 From a biological perspective, the use of key growth traits generated by Leaf-GP can be an excellent
554 tool for screening leaf growth, leaf symmetry, leaf morphogenesis and movement, e.g. phototropism.
555 For example, the leaf skeleton is a useful tool to estimate hyponasty (curvature of the leaf). It could also
556 be used as a marker to quantify plant maturation, e.g. *Arabidopsis* plants transits to the reproductive
557 stage (i.e. flowering), a change from vegetative to flowering meristem when cauline leaves are produced,
558 which can be used to mark differences in maturation. Some traits are also useful in studies other than
559 plant development biology. For instance, vegetative greenness can be used in plant pathogen interaction
560 to analyse the activity of pathogens on the leaf surface, as most of the times broad yellowish symptoms
561 can be observed from susceptible plants (e.g. rust in wheat).

562
563 From a software engineering perspective, we followed best practices in computer vision and image
564 analysis [51] when conducting feature selection, i.e. choosing traits based on the statistical variation or
565 dispersion of a set of phenotypic data values. Whilst implementing the software, we built on our
566 previous work in batch processing and high-throughput trait analysis [52–56] and improved software
567 implementation in areas such as reducing computational complexity (e.g. the usage of CPU cores and
568 memory in parallel computing), optimising data annotation and data exchange between application
569 programming interfaces (APIs), i.e. the objects passing between internal and external functions or
570 procedures, promoting mutual global and local feature verification (e.g. cross validating positional
571 information of plants at the image level as well as the pot level), and implementing software modularity
572 and reusability when packaging the software (see the software executables and package source code in
573 <https://github.com/Crop-Phenomics-Group/Leaf-GP>). Furthermore, we verify that, instead of fully
574 relying on a black-box machine learning approach without an in-depth understanding of why clustering
575 or estimation is accomplished, it is more efficient to establish an analysis algorithm based on a sound
576 knowledge of the biological challenge that we need to address. If the features we are interesting is
577 countable and can be logically described, advanced computer vision and image analysis methods would
578 be efficient for our phenotypic analysis missions.

579

580 **Conclusions**

581 In this paper, we presented Leaf-GP, a comprehensive software application for analysing large growth
582 image series so that multiple growth phenotypes in response to different treatments can be measured
583 and cross-referenced over time. Our software demonstrates that treatment effects such as the response
584 to different temperatures between genotypes could be detected reliably. We demonstrate the usefulness
585 and high accuracy of the software based on the quantification of growth traits for *Arabidopsis* genotypes
586 under varied temperature conditions and wheat growth in the glasshouse over time. To serve a broader
587 plant research community, we improved the usability of the software so that it can be executed on
588 different platforms. To help users or developers to gain an in-depth understanding of the algorithms and
589 the software, we have provided our source code, detailed comments, software modulation strategy, and
590 executables (.exe and .app), together with raw image data and experiment results in the Additional files.
591 The software, source code and experiment results presented in this paper are also freely available at
592 <https://github.com/Crop-Phenomics-Group/Leaf-GP/releases>.

593

594 Leaf-GP package provides an efficient and effective analysis platform for carrying out large growth
595 phenotype measurements with no requirement on programming skills and limited requirements on
596 imaging equipment. We followed the open software strategy so that we could share and contribute
597 jointly with the computational biology community. Our software has confirmed previously reported
598 results in the literature and produces a number of key growth traits that enhance the reproducibility for
599 plant growth studies. Many plant growth and development experiments can be analysed by Leaf-GP
600 under a range of treatment conditions. Our case studies of temperature effects and different genotypes
601 or plant species are not limited. Natural variation in plant growth can also be analysed or images from
602 plants experiencing mineral or nutrient stress could be equally well handled.
603

604 **List of abbreviations**

605 RGB: a red, green and blue colour model
606 NoIR: no infrared filter
607 ROI: regions of interest
608 GUI: graphic user interface
609 HPC: high-performance computer
610 CSV: comma-separated values
611 OS: operating systems
612 CPU: central processing unit
613 Lab: lightness, a for the colour opponents green–red, and b for the colour opponents blue–yellow
614 RGR: relative growth rate
615 *Ler*: Landsberg *erecta* (wildtype)
616 *spt-2*: spatula-2
617 API: application programming interfaces
618

619 **Declarations**

620 **Ethics approval and consent to participate**

621 Not applicable

622

623 **Consent for publication**

624 Not applicable

625

626 **Competing interests**

627 The authors declare no competing financial interests.

628

629 **Authors' contributions**

630 JZ, CA, NP wrote the manuscript, NP, ADA and SO performed the biological experiments under SP
631 and SG's supervision. JZ, NP and DR designed the plant phenotyping protocol. JZ developed and
632 implemented the core analysis algorithm of Leaf-GP. CA, DR and MM implemented and packaged the
633 GUI version under JZ's supervision. JZ, CA and NP tested the software package. NP and JZ performed
634 the data analysis. All authors read and approved the final manuscript.

635

636 **Acknowledgements**

637 The authors would like to thank members of the Zhou laboratory for fruitful discussions. We thank
638 Thomas Le Cornu, Danny Websdale and Jennifer McDonald for excellent technical support and
639 research leaders at EI, JIC, TSL and UEA for constructive discussions. JZ was partially funded by
640 BBSRC's Designing Future Wheat Cross-institute Strategic Programme Grants (BB/P016855/1) to
641 Professor Graham Moore. NP and ADA were supported by a Leverhulme Trust Research Project
642 Grant (CA580-P11-H) awarded to SP. CA was partially supported by BBSRC's FoF award (GP105-
643 JZ1-B) to JZ.

644

645 **Authors' information**

646 ¹Earlham Institute, Norwich Research Park, Norwich UK

647 ²John Innes Centre, Norwich Research Park, Norwich UK

648 ³University of East Anglia, Norwich Research Park, Norwich UK

649

650 **Availability of data and materials**

651 All the 4.3 GB image datasets as well as The Leaf-GP software package and source code are freely
652 available from our online repository <https://github.com/Crop-Phenomics-Group/Leaf-GP/releases>.

653

654 **Open Access**

655 The software is distributed under the terms of the Creative Commons Attribution 4.0 International
656 License (<http://creativecommons.org/licenses/by/4.0/>), which permits unrestricted use, distribution, and
657 reproduction in any medium, provided you give appropriate credit to the original authors and the source,
658 provide a link to the Creative Commons license, and indicate if changes were made. Unless otherwise
659 stated The Creative Commons Public Domain Dedication waiver applies to the data and results made
660 available in this paper.

661

662 **References**

663 1. Scheres B, van der Putten WH. The plant perceptron connects environment to development.

664 Nature. 2017;543:337–45.

665 2. Achard P, Cheng H, De Grauwe L, Decat J, Schoutteten H, Moritz T, et al. Integration of plant

- 666 responses to environmentally activated phytohormonal signals. *Sci.* (New York, NY). 2006;311:91–4.
667 3. Sidaway-Lee K, Josse EM, Brown A, Gan Y, Halliday KJ, Graham IA, et al. SPATULA links
668 daytime temperature and plant growth rate. *Curr. Biol.* Elsevier Ltd; 2010;20:1493–7.
669 4. West C, Briggs GE, Kidd F. *Methods and Significant Relations in the Quantitative Analysis of*
670 *Plant Growth.* New Phytol. 1920;19:200–7.
671 5. Tessmer OL, Jiao Y, Cruz JA, Kramer DM, Chen J. Functional approach to high-throughput plant
672 growth analysis. *BMC Syst. Biol.* 2013;7:S17.
673 6. Malosetti M, Ribaut JM, Vargas M, Crossa J, Van Eeuwijk FA. A multi-trait multi-environment
674 QTL mixed model with an application to drought and nitrogen stress trials in maize (*Zea mays* L.).
675 *Euphytica.* 2008;161:241–57.
676 7. Junker A, Muraya MM, Weigelt-Fischer K, Arana-Ceballos F, Klukas C, Melchinger AE, et al.
677 Optimizing experimental procedures for quantitative evaluation of crop plant performance in high
678 throughput phenotyping systems. *Front. Plant Sci.* 2015;5:770.
679 8. Bourdais G, Burdiak P, Gauthier A, Nitsch L, Salojrvi J, Rayapuram C, et al. Large-Scale
680 Phenomics Identifies Primary and Fine-Tuning Roles for CRKs in Responses Related to Oxidative
681 Stress. *PLoS Genet.* 2015;11:1–36.
682 9. Zhu J, van der Werf W, Anten NPR, Vos J, Evers JB. The contribution of phenotypic plasticity to
683 complementary light capture in plant mixtures. *New Phytol.* 2015;207:1213–22.
684 10. Turc O, Bouteill M, Fuad-Hassan A, Welcker C, Tardieu F. The growth of vegetative and
685 reproductive structures (leaves and silks) respond similarly to hydraulic cues in maize. *New Phytol.*
686 2016;212:377–88.
687 11. Borrell AK, van Oosterom EJ, Mullet JE, George-Jaeggli B, Jordan DR, Klein PE, et al. Stay-
688 green alleles individually enhance grain yield in sorghum under drought by modifying canopy
689 development and water uptake patterns. *New Phytol.* 2014;203:817–30.
690 12. Walter A, Scharr H, Gilmer F, Zierer R, Nagel KA, Ernst M, et al. Dynamics of seedling growth
691 acclimation towards altered light conditions can be quantified via GROWSCREEN: A setup and
692 procedure designed for rapid optical phenotyping of different plant species. *New Phytol.*
693 2007;174:447–55.
694 13. Meyer GE, Neto JC. Verification of color vegetation indices for automated crop imaging
695 applications. *Comput. Electron. Agric.* 2008;63:282–93.
696 14. Eliceiri K, Berthold M, Goldberg I, Ibáñez L, Manjunath B, Martone ME, et al. Biological
697 imaging software tools. *Nat. Methods.* 2012 Jan.
698 15. Boyes DC. Growth Stage-Based Phenotypic Analysis of Arabidopsis: A Model for High
699 Throughput Functional Genomics in Plants. *Plant Cell Online.* 2001;13:1499–510.
700 16. Klukas C, Chen D, Pape J-M. Integrated Analysis Platform: An Open-Source Information System
701 for High-Throughput Plant Phenotyping. *Plant Physiol.* 2014;165:506–18.
702 17. Cardona A, Tomancak P. Current challenges in open-source bioimage informatics. *Nat. Methods.*
703 Nature Publishing Group; 2012;9:661–5.
704 18. Weight C, Parnham D, Waites R. LeafAnalyser: A computational method for rapid and large-scale
705 analyses of leaf shape variation. *Plant J.* 2008;53:578–86.
706 19. Jansen M, Gilmer F, Biskup B, Nagel KA, Rascher U, Fischbach A, et al. Simultaneous
707 phenotyping of leaf growth and chlorophyll fluorescence via Growscreen Fluoro allows detection of
708 stress tolerance in Arabidopsis thaliana and other rosette plants. *Funct. Plant Biol.* 2009;36:902–14.
709 20. Arvidsson S, Pérez-Rodríguez P, Mueller-Roeber B. A growth phenotyping pipeline for
710 Arabidopsis thaliana integrating image analysis and rosette area modeling for robust quantification of
711 genotype effects. *New Phytol.* 2011;191:895–907.
712 21. Dhondt S, Van Haerenborgh D, Van Cauwenbergh C, Merks RMH, Philips W, Beemster GTS, et
713 al. Quantitative analysis of venation patterns of Arabidopsis leaves by supervised image analysis.
714 *Plant J.* 2012;69:553–63.
715 22. De Vylder J, Vandenbussche F, Hu Y, Philips W, Van Der Straeten D. Rosette Tracker: An Open
716 Source Image Analysis Tool for Automatic Quantification of Genotype Effects. *Plant Physiol.*
717 2012;160:1149–59.
718 23. Green JM, Appel H, Rehrig EM, Harnsomburana J, Chang J-F, Balint-Kurti P, et al. PhenoPhyte:
719 a flexible affordable method to quantify 2D phenotypes from imagery. *Plant Methods.* 2012;8:45.
720 24. Bours R, Muthuraman M, Bouwmeester H, van der Krol A. OSCILLATOR: A system for analysis

- 721 of diurnal leaf growth using infrared photography combined with wavelet transformation. *Plant*
722 *Methods*. 2012;8:29.
- 723 25. Maloof JN, Nozue K, Mumbach MR, Palmer CM. LeafJ: An ImageJ Plugin for Semi-automated
724 Leaf Shape Measurement. *J. Vis. Exp.* 2013;2–7.
- 725 26. Easlon HM, Bloom AJ. Easy Leaf Area: Automated Digital Image Analysis for Rapid and
726 Accurate Measurement of Leaf Area. *Appl. Plant Sci.* 2014;2:1400033.
- 727 27. Apelt F, Breuer D, Nikoloski Z, Stitt M, Kragler F. Phytotyping 4D: A light-field imaging system
728 for non-invasive and accurate monitoring of spatio-temporal plant growth. *Plant J.* 2015;82:693–706.
- 729 28. Müller-Linow M, Pinto-Espinosa F, Schar H, Rascher U. The leaf angle distribution of natural
730 plant populations: assessing the canopy with a novel software tool. *Plant Methods*. 2015;11:11.
- 731 29. Biot E, Cortizo M, Burguet J, Kiss A, Oughou M, Maugarny-Calès A, et al. Multiscale
732 quantification of morphodynamics: MorphoLeaf software for 2D shape analysis. *Development*.
733 2016;143:3417–28.
- 734 30. Tomé F, Jansseune K, Saey B, Grundy J, Vandenbroucke K, Hannah MA, et al. rosettaR: protocol
735 and software for seedling area and growth analysis. *Plant Methods*. *BioMed Central*; 2017;13:13.
- 736 31. Naik HS, Zhang J, Lofquist A, Assefa T, Sarkar S, Ackerman D, et al. A real-time phenotyping
737 framework using machine learning for plant stress severity rating in soybean. *Plant Methods*. *BioMed*
738 *Central*; 2017;13:23.
- 739 32. Zhou J, Reynolds D, Corn T Le, Websdale D, Gonzalez-Navarro O, Lister C, et al. CropQuant:
740 The next-generation automated field phenotyping platform for breeding and digital agriculture.
741 *bioRxiv* [Internet]. 2017;1–25. Available from:
742 <http://www.biorxiv.org/content/early/2017/07/10/161547.article-metrics>
- 743 33. Millman KJ, Aivazis M. Python for scientists and engineers. *Comput. Sci. Eng.* 2011;13:9–12.
- 744 34. van der Walt S, Schönberger JL, Nunez-Iglesias J, Boulogne F, Warner JD, Yager N, et al. Scikit-
745 image: image processing in Python. *PeerJ.* 2014;2:1–18.
- 746 35. Howse J. *OpenCV Computer Vision with Python*. 1st ed. Birmingham, UK: Packt Publishing
747 Ltd.; 2013.
- 748 36. Pedregosa F, Varoquaux G, Gramfort A, Michel V, Thirion B, Grisel O, et al. Scikit-learn:
749 Machine Learning in Python. *J. Mach. Learn. Res.* 2011;12:2825–30.
- 750 37. Shipman JW. Tkinter 8.5 reference: a GUI for Python [Internet]. New Mex. Tech - Comput. Cent.
751 New Mexico; 2013. Available from: tcc-doc@nmt.edu
- 752 38. Kruchten P. What Is the Rational Unified Process? *Ration. Softw.* 2003. 2003;3:11–23.
- 753 39. Smith JR, Chang S. Single Color Extraction and Image Query. *Int. Conf. Image Process.*
754 Washington, DC: ICIP-95; 1995. p. 1–4.
- 755 40. Otsu N. A threshold selection method from gray-level histograms. *IEEE Trans. Syst. Man Cybern.*
756 1979;1:62–6.
- 757 41. McLAREN K. XIII—The Development of the CIE 1976 ($L^* a^* b^*$) Uniform Colour Space and
758 Colour-difference Formula. *J. Soc. Dye. Colour.* 1976;92:338–41.
- 759 42. Peli E. In search of a contrast metric: Matching the perceived contrast of gabor patches at different
760 phases and bandwidths. *Vision Res.* 1997;37:3217–24.
- 761 43. Flusser J, Member S. Rotation Moment Invariants for Recognition of Symmetric Objects. *IEEE*
762 *Trans. Image Process.* 2006;15:3784–90.
- 763 44. Manjunath BS, Ohm JR, Vasudevan V V., Yamada A. Color and texture descriptors. *IEEE Trans.*
764 *Circuits Syst. Video Technol.* 2001;11:703–15.
- 765 45. Leister D, Varotto C, Pesaresi P, Niwergall A, Salamini F. Large-scale evaluation of plant growth
766 in *Arabidopsis thaliana* by non-invasive image analysis. *Plant Physiol. Biochem.* 1999. p. 671–8.
- 767 46. Hoffmann WA, Poorter H. Avoiding bias in calculations of relative growth rate. *Ann. Bot.*
768 2002;90:37–42.
- 769 47. Preparata FP, Hong SJ. Convex hulls of finite sets of points in two and three dimensions.
770 *Commun. ACM.* 1977;20:87–93.
- 771 48. Bergman S. *Open analytic_wfm.py* [Internet]. Github; 2017. Available from:
772 <https://gist.github.com/sixtenbe/1178136>
- 773 49. Tsiftaris SA, Minervini M, Schar H. Machine Learning for Plant Phenotyping Needs Image
774 Processing. *Trends Plant Sci.* Elsevier Ltd; 2016;21:989–91.
- 775 50. Grime JP, Hunt R. Relative growth rate: its range and adaptive significance in a local flora. *J.*

- 776 Ecol. 1975;63:393–422.
777 51. Petrou M, Petrou C. Image processing: the fundamentals. second edi. Singapore: Wiley; 2010.
778 52. Faulkner C, Zhou J, Evrard A, Bourdais G, MacLean D, Häweker H, et al. An automated
779 quantitative image analysis tool for the identification of microtubule patterns in plants. *Traffic*.
780 2017;11:109–17.
781 53. Meteignier L, Zhou J, Cohen M, Bhattacharjee S, Brosseau C. NB-LRR signaling induces
782 translational repression of viral transcripts and the formation of RNA processing bodies through
783 mechanisms differing from those activated by UV stress and RNAi. *J. Exp. Bot.* 2016;67:1–14.
784 54. Zhou J, Spallek T, Faulkner C, Robatzek S. CalloseMeasurer: a novel software solution to
785 measure callose deposition and recognise spreading callose patterns. *Plant Methods*. *Plant Methods*;
786 2013;8:49.
787 55. Beck M, Zhou J, Faulkner C, MacLean D, Robatzek S. Spatio-temporal cellular dynamics of the
788 Arabidopsis flagellin receptor reveal activation status-dependent endosomal sorting. *Plant Cell*.
789 2012;24:4205–19.
790 56. Fitzgibbon J, Beck M, Zhou J, Faulkner C, Robatzek S, Oparka K. A Developmental Framework
791 for Complex Plasmodesmata Formation Revealed by Large-Scale Imaging of the Arabidopsis Leaf
792 Epidermis. *Plant Cell Online*. 2013;25:57–70.
793

794 **Additional files**

- 795 • **Additional File 1:** The interactive *Jupyter Notebook version* for Leaf-GP (version 1.18)
- 796 • **Additional File 2:** Install manual for Python environment, Anaconda Python distribution and
797 OpenCV-Python binding
- 798 • **Additional File 3:** Processed images of *Arabidopsis* rosettes at different growth stages
- 799 • **Additional File 4:** Multiple trait measurements results based on a testing series
- 800 • **Additional File 5:** The analysis workflow and a detailed activity diagram of Leaf-GP
- 801 • **Additional File 6:** The manual for importing image datasets via the GUI version of Leaf-GP
- 802 • **Additional File 7:** The *Jupyter Notebook version* for plotting and cross-referencing growth traits
803 between experiments
- 804 • **Additional File 8:** Multiple trait measurements results based on *Ler* 12°C, 17°C, 22°C
- 805 • **Additional File 9:** Multiple trait measurements results based on *spt-2* 12°C, 17°C, 22°C
806

807 **Figures Legends**

808 **Figure 1. An overview of how to utilise Leaf-GP in plant growth research.**

809 (a-c) A range of imaging devices, including a fixed imaging platform, smartphones, or a mobile version
810 CropQuant equipped with either a *Pi* NoIR sensor or an RGB sensor. (d-e) The regions of a tray or a
811 pot need to be covered. (f-g) Both raw and processed image data can be loaded and saved by Leaf-GP
812 on PCs, HPC clusters, or cloud-based computing storage. (h-j) Three versions of Leaf-GP, including
813 HPC, GUI and a *Jupyter Notebook*. (k-l) Processed images highlighting key growth phenotypes and
814 CSV files containing trait measurements are produced after the batch image processing.
815

816 **Figure 2. The analysis workflow and the GUI of Leaf-GP.**

817 (a) The high-level analysis workflow of Leaf-GP contains five main steps. (b) Five self-explanatory
818 sections designed to integrate the analysis workflow into the GUI version of Leaf-GP. (c) The initial
819 status of the GUI. (d) The screenshot after selecting image series. (e) The screenshot when image
820 datasets are being processed in parallel. (f) Growth-related trait plots can be generated by clicking the
821 associated cell in the Results table.
822

823 **Figure 3. The step of image pre-processing and calibration.**

824 (a-b) Fix the height (i.e. y-axis) of all images in a given series. (c) Detect red circular markers. (d)
825 Extract ROI from the original image. (e) Denoise the image to smooth leaf surface for the global leaf
826 segmentation.
827

828 **Figure 4. The step of defining global leaf ROI.**

829 (a-d) A number of experiment-related problems encountered whilst developing Leaf-GP (to the left of
830 the figures) and results of our solutions (to the right of figures). (e) A pseudo vegetative greenness
831 image. (f-g) Using KMeans to estimate how many colour groups can be classified from a given colour
832 image. (h) The classification result of the KMeans approach based on the pseudo vegetative greenness
833 picture, highlighting greenness values in red pixels. (i) A global adaptive Otsu thresholding used to
834 generate a global leaf ROI binary mask. (j-k) Lab colour space used to extract leaf ROI objects at the
835 image level.
836

837 **Figure 5. The step of conducting pot level segmentation in a sequential manner.**

838 (a) Depending on the number of rows and columns, generate anti-aliased lines to define the pot layout.
839 (b) Segmented a given image into a number of sub-images. (c) The sequence to go through each pot an
840 in an iterative approach. (d-e) Apply a local detection method to improve the result of leaf detection.
841

842 **Figure 6. The step of measuring multiple growth traits.**

843 (a) Refined leaf masks for every pot. (b) Contours generated to outline the leaf region. (c) Green pixels
844 enclosed by the contours are totalled for computing the size of the projected leaf area. (d) Convex hulls
845 created in every pot for calculating leaf canopy. (e) Stockiness calculated based on the ratio between
846 the plant projected area and the leaf perimeter. (f) Leaf Compactness computed based on the ratio
847 between the projected leaf area and the area of the convex hull.
848

849 **Figure 7. The step of detecting leaf structure.**

850 (a) The result of a 2D skeletonisation approach to extract leaf structure. (b) Detect end points of the leaf
851 structure which correlates with leaf tips. (c) Large or long rosette leaves identified if they are over 50%
852 or 70% of the final size. (d-e) Generate a distance series to represent the distance between the plant
853 centroid and its leaf contour, at angles between 0 and 359 degrees with a 15-degree interval. (f-g) The
854 number of detected peaks are used to represent the number of leaf tips.
855

856 **Figure 8. Case study 1: Analysis results of a tray with three genotypes**

857 (a) The projected leaf area trait in 24 pots was quantified by Leaf-GP. (b) The projected leaf area traits
858 divided into three genotype groups. (c-f) A number of growth related traits such as leaf perimeter,
859 compactness, leaf number, and daily RGR of all three genotypes can be statistically differentiated.
860

861 **Figure 9. Case Study 2: Analysis results of multiple experiments**

862 (a) The projected leaf area measurements used to observe how temperatures affect vegetative growth
863 on both *Ler* and *spt-2*. (b) Plants of both genotypes growing at 12°C had more compact rosettes that
864 those growing at 17°C. *spt-2* was less compact than *Ler* in general. (c) The number of leaves produced
865 was greater at the warmer temperature.
866

867 **Figure 10. Case Study 3: Applying Leaf-GP on wheat growth studies**

868 (a) A proof-of-concept study of how to measure the projected leaf area and the leaf canopy size based
869 on *Paragon* wheat images, taken over a 70-day period in greenhouse. (b-f) Analysis results generated
870 from sprouting to heading stage.

Figure 2. The GUI of Leaf-GP

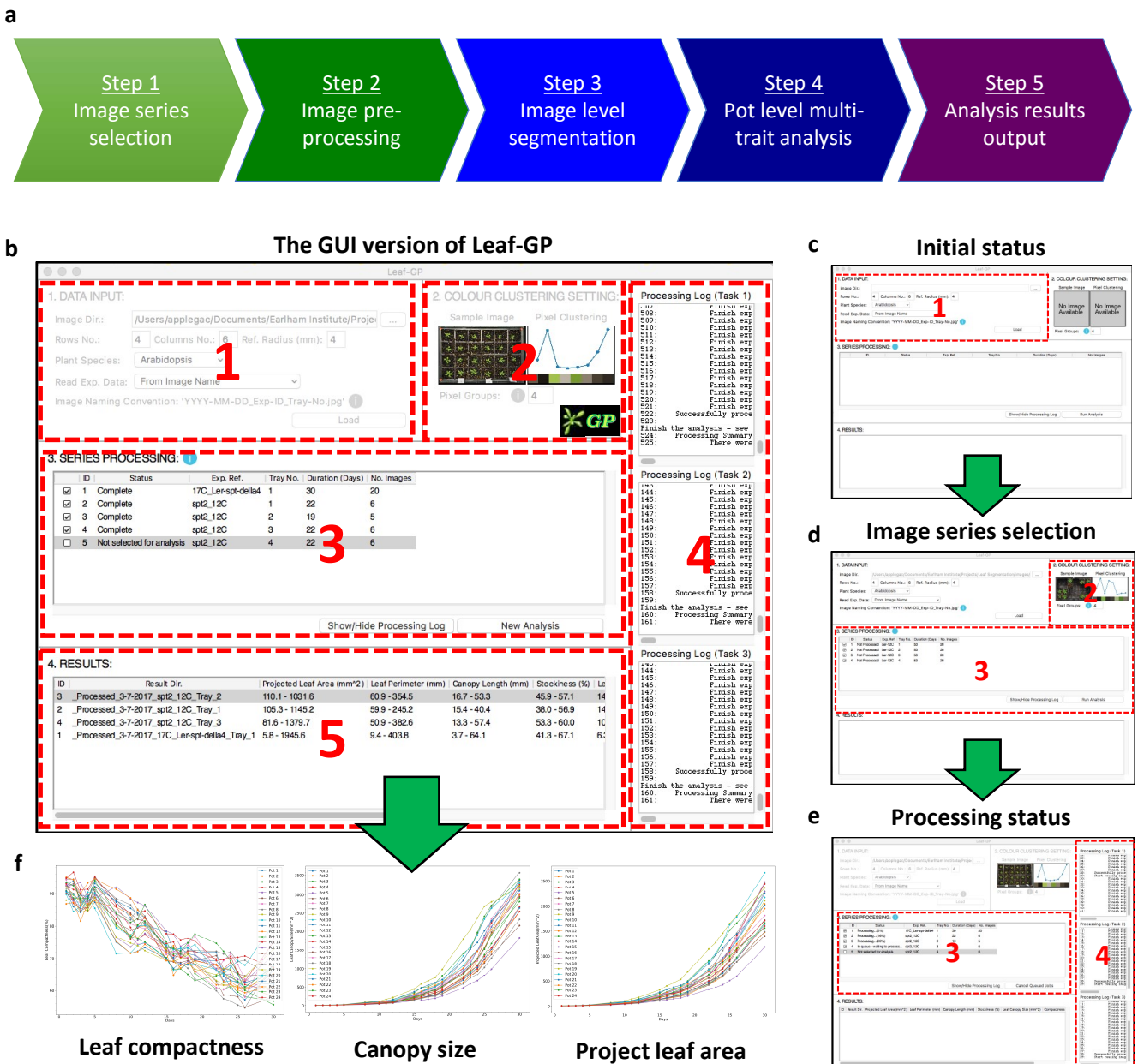


Figure 3. Image Preprocessing and Calibration

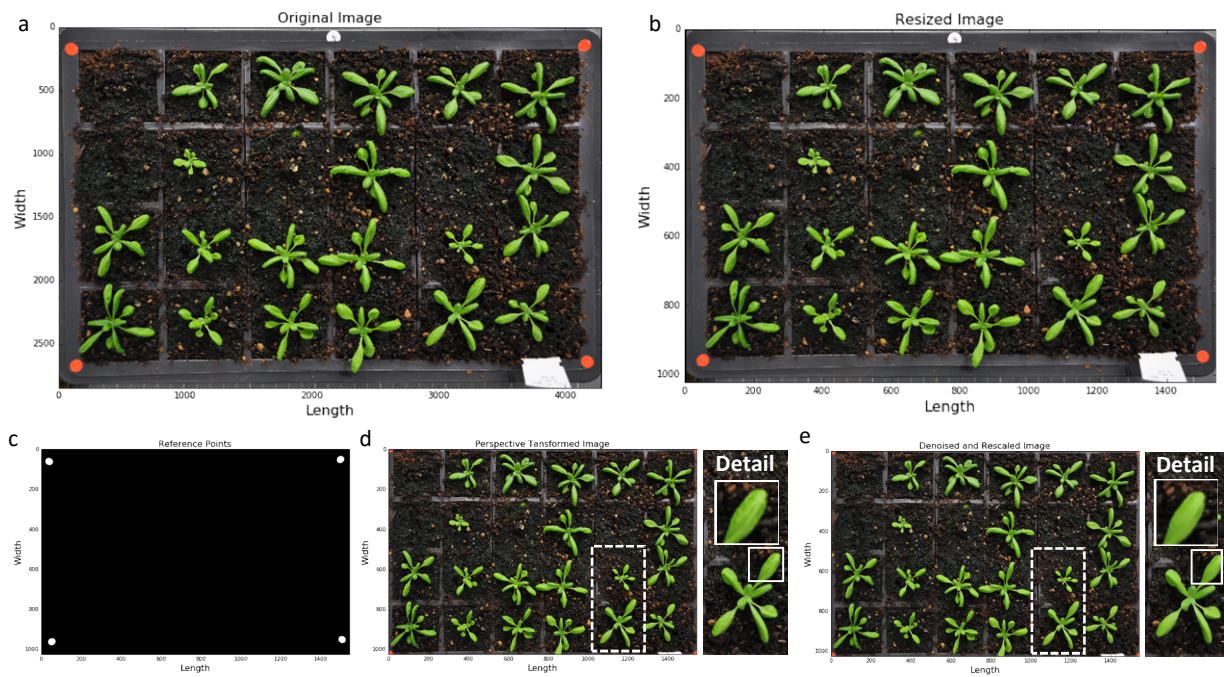


Figure 4. Define global leaf ROI

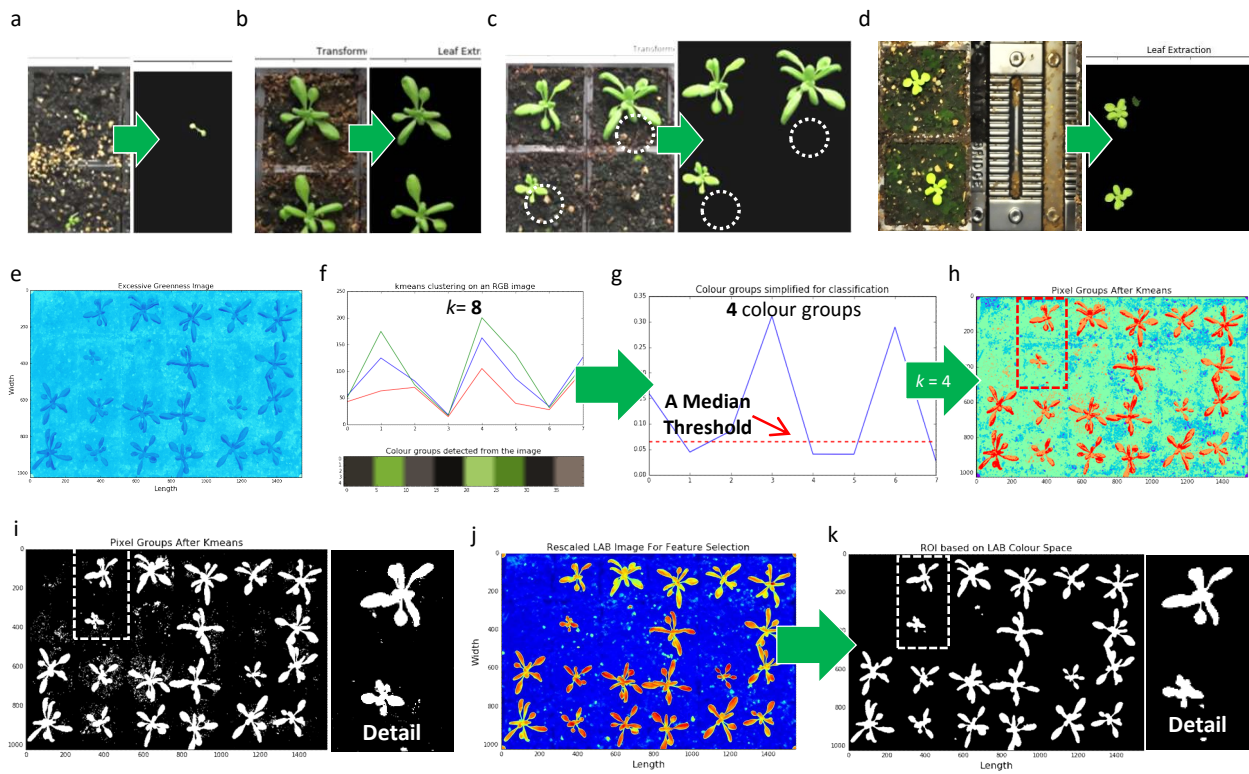


Figure 5. Conducting sequential pot level segmentation

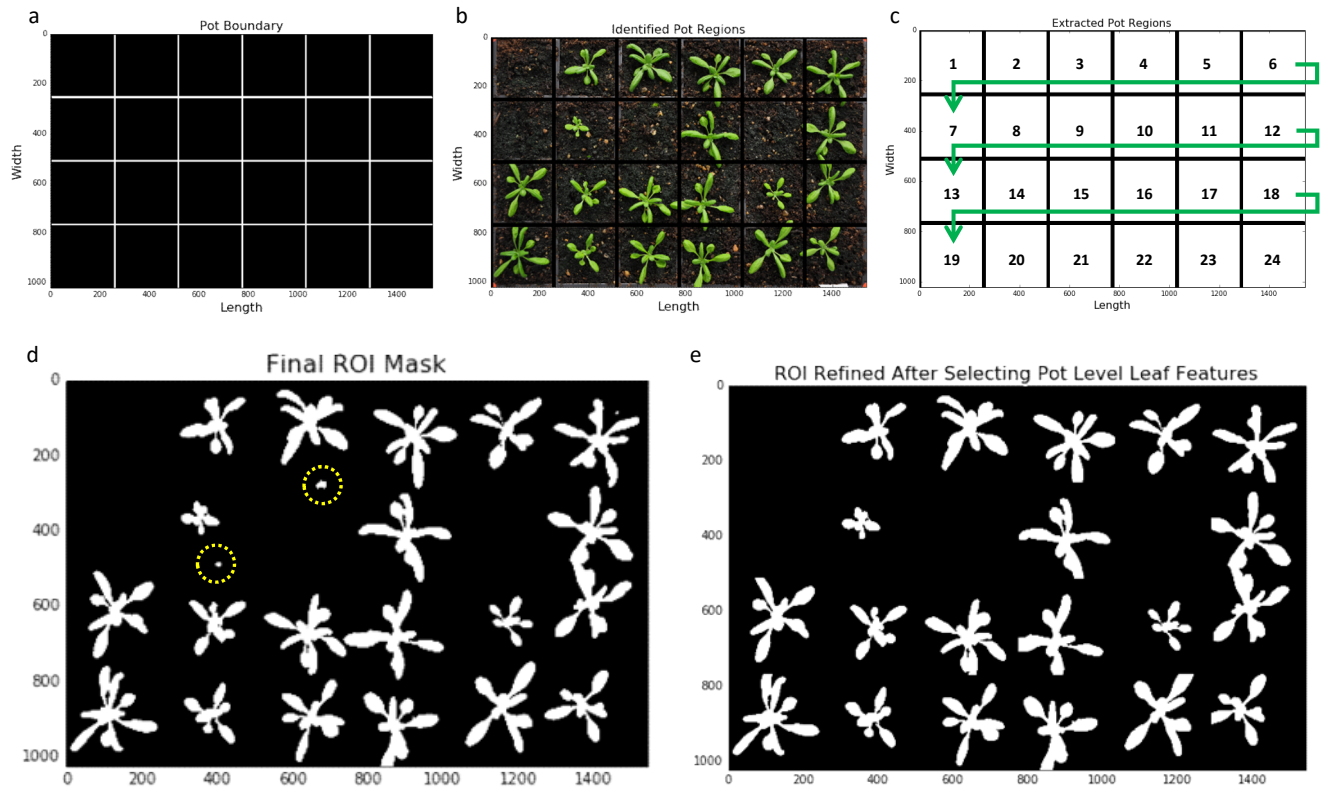


Figure 6. Local multiple trait measurements

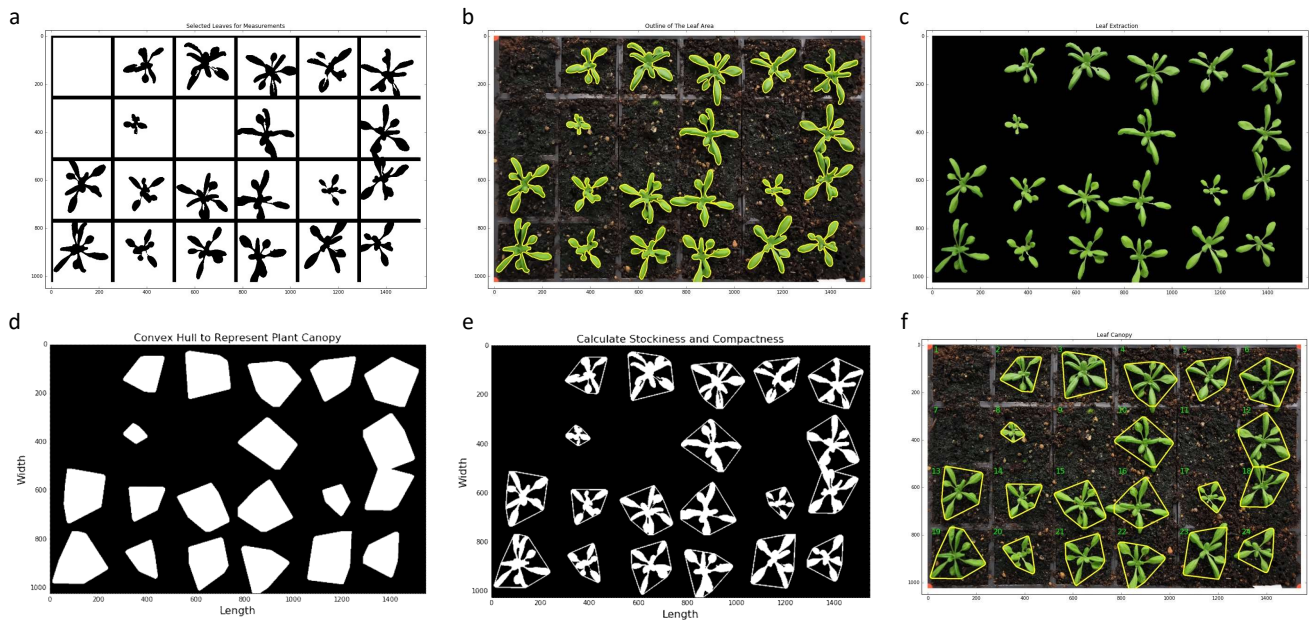


Figure 7. Leaf structure detection

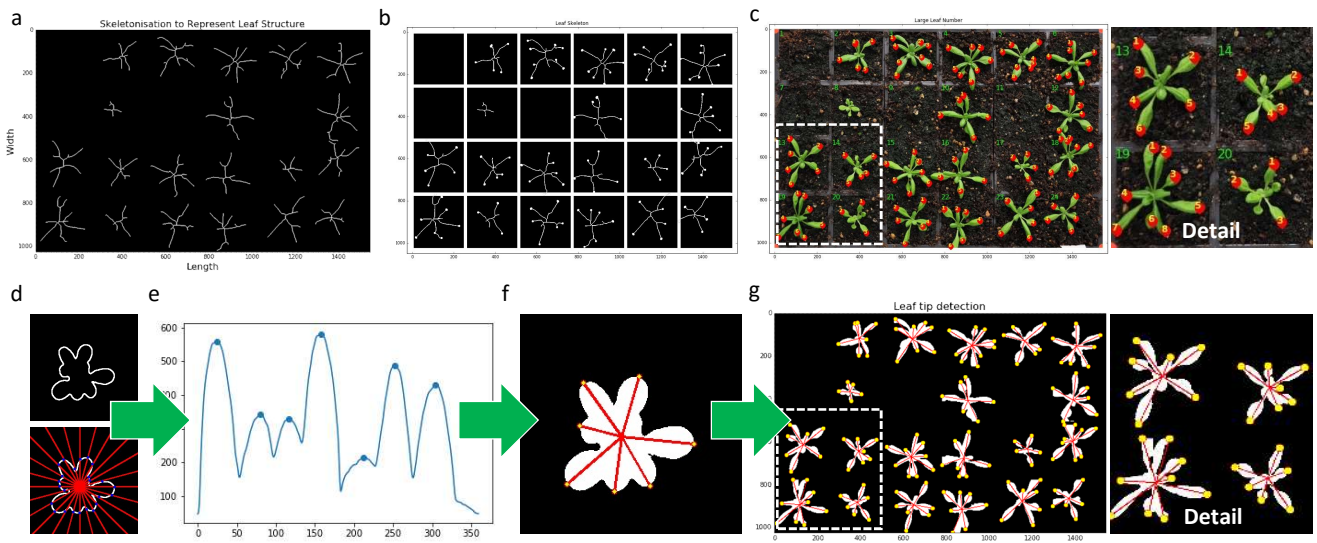


Figure 8. Case study 1: Analysis results of a tray with three genotypes

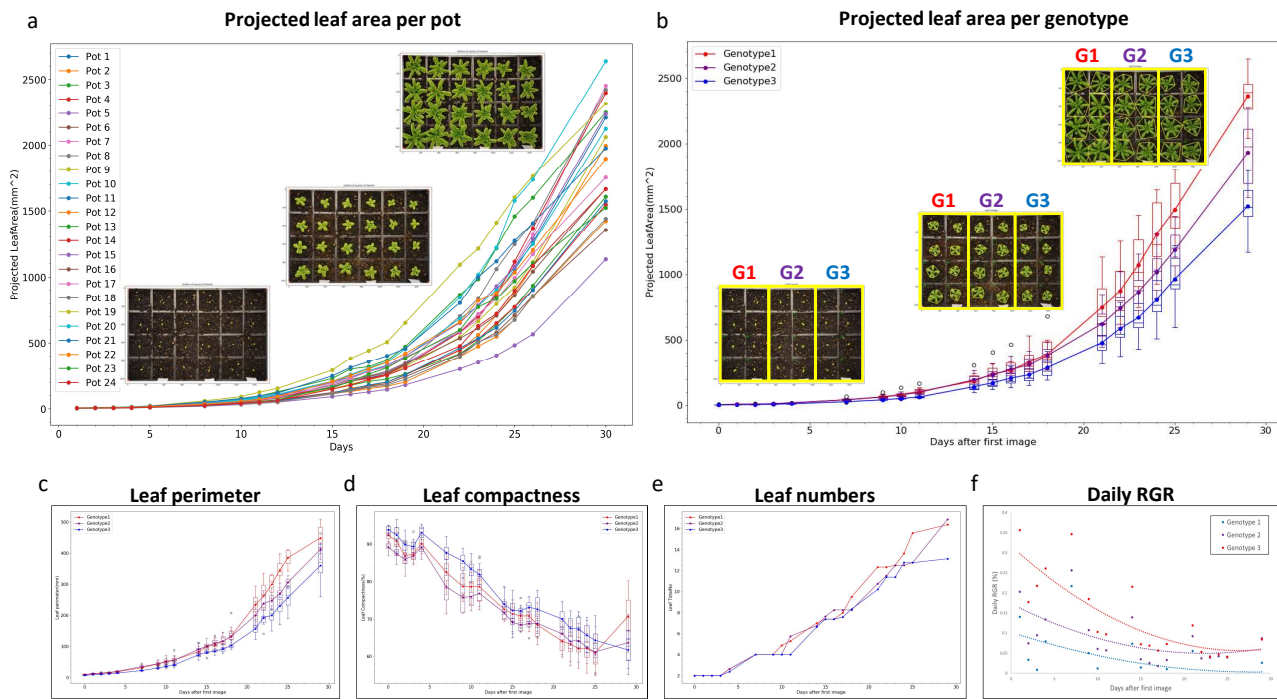


Figure 9. Case Study 2 – Analysis results of multiple experiments

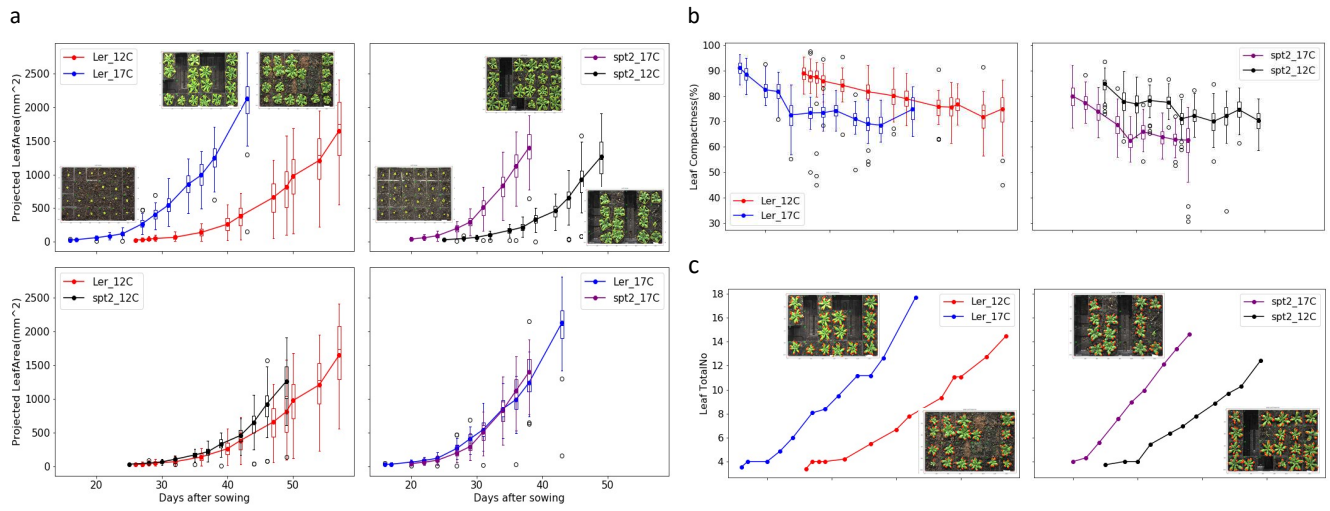
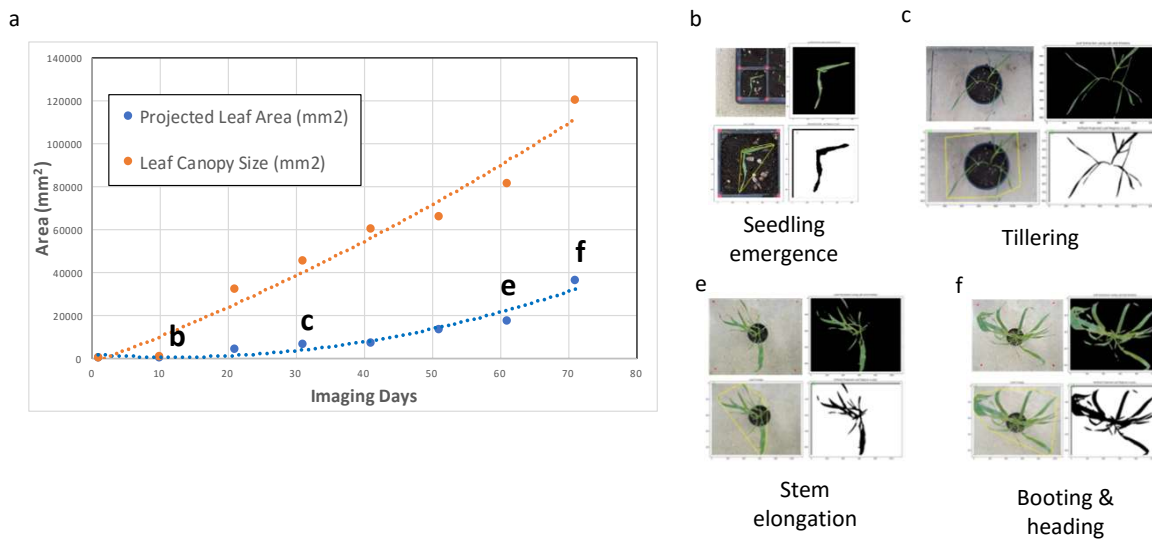
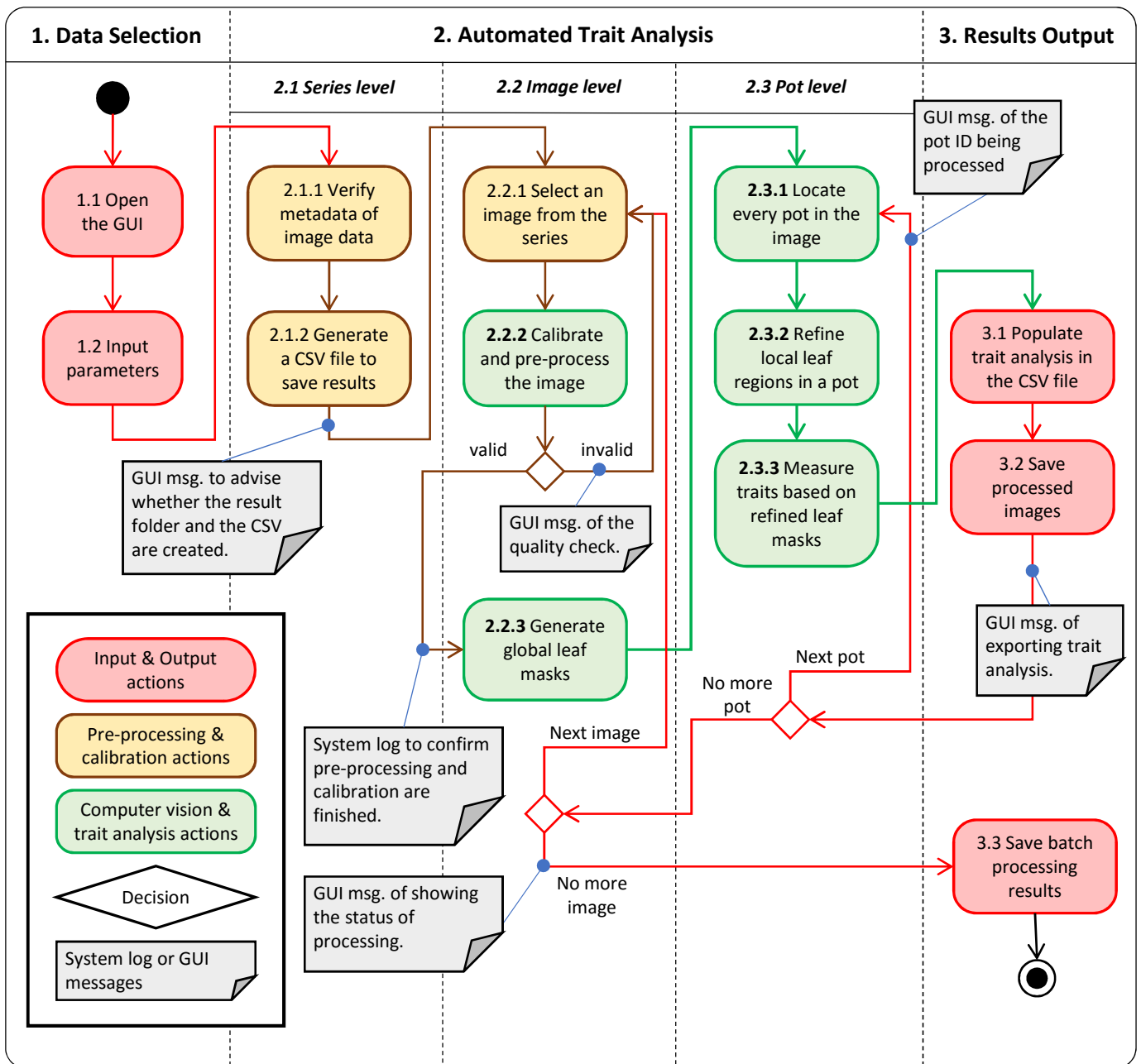


Figure 10. Case Study 3 – Application on Wheat



Supplemental Figure 1. The Analysis Workflow of Leaf-GP



Supplemental Figure 2. The GUI operation

a

1. DATA INPUT: Image Dir.: Rows No.: 4 Columns No.: 6 Ref. Radius (mm): 4 Plant Species: Arabidopsis Read Exp. Date: From Image Name Image Naming Convention: YYYY-MM-DD_Exp-ID_Tray-No.jpg

2. COLOUR CLUSTERING SETTING: Sample Image Pixel Clustering No Image Available No Image Available Pixel Groups: 1, 4

3. SERIES PROCESSING:

ID	Status	Exp. Ref.	Tray No.	Duration (Days)	No. Images
1	Not Processed	Lar-12C	1	53	20
2	Not Processed	Lar-12C	2	53	20
3	Not Processed	Lar-12C	3	53	20
4	Not Processed	Lar-12C	4	53	20

4. RESULTS:

Processing status

b

1. DATA INPUT: Image Dir.: /Users/applejac/Documents/Earham Institute/Projects/Leaf Segmentation/images/ Rows No.: 4 Columns No.: 6 Ref. Radius (mm): 4 Plant Species: Arabidopsis Read Exp. Date: From Image Name Image Naming Convention: YYYY-MM-DD_Exp-ID_Tray-No.jpg

2. COLOUR CLUSTERING SETTING: Sample Image Pixel Clustering Pixel Groups: 1, 4

3. SERIES PROCESSING:

ID	Status	Exp. Ref.	Tray No.	Duration (Days)	No. Images
1	Not Processed	Lar-12C	1	53	20
2	Not Processed	Lar-12C	2	53	20
3	Not Processed	Lar-12C	3	53	20
4	Not Processed	Lar-12C	4	53	20

4. RESULTS:

Results visualisation

c

1. DATA INPUT: Image Dir.: /Users/applejac/Documents/Earham Institute/Projects/ Leaf Segmentation/images/ Rows No.: 4 Columns No.: 6 Ref. Radius (mm): 4 Plant Species: Arabidopsis Read Exp. Date: From Image Name Image Naming Convention: YYYY-MM-DD_Exp-ID_Tray-No.jpg

2. COLOUR CLUSTERING SETTING: Sample Image Pixel Clustering Pixel Groups: 1, 4

3. SERIES PROCESSING:

ID	Status	Exp. Ref.	Tray No.	Duration (Days)	No. Images
1	Processing... (5%)	17C_Lar-seg-delB4	1	30	20
2	Processing... (16%)	sp2_12C	1	22	6
3	Processing... (20%)	sp2_12C	2	19	5
4	In queue - waiting to process.	sp2_12C	3	6	6
5	Not selected for analysis	sp2_12C	4	22	6

4. RESULTS:

ID	Result Dir.	Projected Leaf Area (mm ²)	Leaf Perimeter (mm)	Canopy Length (mm)	Stinkiness (N)	Leaf Canopy Size (mm ²)	Connectivity
1	Processed 3-7-2017_17C_Lar-seg-delB4_Tray_1	110.1-1031.6	609-3545	167-533	45.9-57.1	14	14
2	Processed 3-7-2017_sp2_12C_Tray_1	105.3-1145.2	589-2462	154-404	38.0-56.9	14	14
3	Processed 3-7-2017_sp2_12C_Tray_2	81.6-1237.7	609-382.6	103-174	32.3-60.0	1C	1C
4	Processed 3-7-2017_17C_Lar-seg-delB4_Tray_1	5.8-1945.6	94-403.8	3.7-84.1	41.3-67.1	6C	6C

d

1. DATA INPUT: Image Dir.: /Users/applejac/Documents/Earham Institute/Projects/ Leaf Segmentation/images/ Rows No.: 4 Columns No.: 6 Ref. Radius (mm): 4 Plant Species: Arabidopsis Read Exp. Date: From Image Name Image Naming Convention: YYYY-MM-DD_Exp-ID_Tray-No.jpg

2. COLOUR CLUSTERING SETTING: Sample Image Pixel Clustering Pixel Groups: 1, 4

3. SERIES PROCESSING:

ID	Status	Exp. Ref.	Tray No.	Duration (Days)	No. Images
1	Complete	17C_Lar-seg-delB4	1	30	20
2	Complete	sp2_12C	1	22	6
3	Complete	sp2_12C	2	19	5
4	Complete	sp2_12C	3	22	6
5	Not selected for analysis	sp2_12C	4	22	6

4. RESULTS:

ID	Result Dir.	Projected Leaf Area (mm ²)	Leaf Perimeter (mm)	Canopy Length (mm)	Stinkiness (N)	Leaf Canopy Size (mm ²)	Connectivity
1	Processed 3-7-2017_17C_Lar-seg-delB4_Tray_1	110.1-1031.6	609-3545	167-533	45.9-57.1	14	14
2	Processed 3-7-2017_sp2_12C_Tray_1	105.3-1145.2	589-2462	154-404	38.0-56.9	14	14
3	Processed 3-7-2017_sp2_12C_Tray_2	81.6-1237.7	609-382.6	103-174	32.3-60.0	1C	1C
4	Processed 3-7-2017_17C_Lar-seg-delB4_Tray_1	5.8-1945.6	94-403.8	3.7-84.1	41.3-67.1	6C	6C